A Route to Diverse Combinatorial Libraries of Electroactive Nickel Hexacyanoferrate

William A. Steen and Daniel T. Schwartz*

Electrochemical Materials and Interfaces Laboratory, Department of Chemical Engineering, University of Washington, Seattle, Washington 98195

Received November 25, 2002. Revised Manuscript Received April 9, 2003

Electroactive nickel hexacyanoferrate (NiHCF) thin films are of interest for their ion sensing and ion intercalation properties; these properties depend on the material's stoichiometry and structure. A small combinatorial library of NiHCF thin films was synthesized by microdispensing 2-μL droplets of reagent with varied proportions of a divalent nickel source (nickel sulfate), a ferricyanide source (potassium ferricyanide), and water on Pt substrates. Two different mixing orders were used ($Ni^{II}/H_2O/Fe^{III}$ and $Fe^{III}/H_2O/Ni^{II}$) and 13 discrete compositions on the ternary reagent diagram were chosen. These 26 library members were electrochemically intercalated/deintercalated with K^+ ions by cyclic voltammetry. Raman spectroscopy was used to screen individual library members for electroactivity; this step eliminated 11 inactive members, most of which resulted from Ni^{II}-rich growth conditions. Energy-dispersive X-ray spectroscopy (EDS) was used to determine the number of intercalated K^+ ions in the oxidized unit cell ($N_{K,ox}$) for the remaining 15 members. The quantity $N_{K,ox}$ is a sensitive measure of NiHCF matrix stoichiometry, with a perfectly stoichiometric matrix possessing $N_{K,ox} = 4$. $N_{K,ox}$ for this library was found to vary from 0 to ~3 (maximum possible variability is 0−4), with smaller $N_{K,ox}$ from the $Ni^{II}/H_2O/Fe^{III}$ mixing order and larger $N_{K,ox}$ from the $Fe^{III}/H_2O/Ni^{II}$ order. The methods used to synthesize this small, but diverse, library are easily scalable to much larger libraries.

Introduction

For 2 decades, electroactive nickel hexacyanoferrate (NiHCF) thin films have been explored as derivatization layers for electrochemical sensing of aqueous alkali cations.[1−7] More recently, electroactive NiHCF has generated interest as a highly cesium-selective ion exchange matrix that can be electrochemically regenerated by oxidation of iron centers in the solid.[8−11] These applications for electroactive NiHCF thin films rely on the material's differential selectivity for various Group I cations and, for the case of separations, the electrochemical regeneration efficiency of the matrix (i.e., how thoroughly the matrix deintercalates ions upon oxidation).[12] The selectivity of electroactive NiHCF has been attributed, for some time, to the nature of solvent exclusion from the zeolite-like NiHCF matrix.[4,13] Recent molecular simulations[14] and X-ray spectroscopy studies[15,16] have shown the primary roles that both ion and solvent size-exclusion effects play in polycrystalline NiHCF thin films. Moreover, regeneration efficiency is directly tied to the matrix stoichiometry. In short, a host of key cation intercalation properties are dictated by the matrix structure and stoichiometry.

The stoichiometry and structure of bulk NiHCF powders has been shown to be highly tunable, ranging from $K_{1.36}Ni_{1.07}Fe(CN)_6$ to $K_{0.03}Ni_{1.81}Fe(CN)_6$ for the (nominally) reduced potassium form of the powder.[17] The dozens of recipes reported by Loos-Neskovic for synthesizing bulk NiHCF powders indicate that material diversity can be controlled by varying the aqueous composition of the ferri-/ferrocyanide and divalent nickel solutions, as well as changing the mixing order (adding Ni^{2+} into $Fe(CN)_6^{-3/-4}$ or vice versa) and the degree of

(1) Amos, L. J.; Schmidt, M. H.; Sinha, S.; Bocarsly, A. B. *Langmuir* **1986**, *2*, 559−561.
(2) Amos, L. J.; Duggal, A.; Mirsky, E. J.; Ragonesi, P.; Bocarsly, A. B.; Bocarsly, P. A. F. *Anal. Chem.* **1988**, *60*, 245−249.
(3) Humphrey, B. D.; Sinha, S.; Bocarsley, A. B. *J. Phys. Chem* **1984**, *88*, 736−743.
(4) Schneemeyer, L. F.; Spengler, S. E.; Murphy, D. W. *Inorg. Chem.* **1985**, *24*, 3044−3046.
(5) Kelly, M. T.; Arbuckle-Keil, G. A.; Johnson, L. A.; Su, E. Y.; Amos, L. J.; Chun, J. K. M.; Bocarsly, A. B. *J. Electroanal. Chem.* **2001**, *500*, 311−321.
(6) Wu, Y.; Pfennig, B. W.; Bocarsly, A. B.; Vicenzi, E. P. *Inorg. Chem.* **1995**, *34*, 4262−4267.
(7) Humphrey, B. D.; Sinha, S.; Bocarsley, A. B. *J. Phys. Chem.* **1987**, *91*, 586−593.
(8) Rassat, S. D.; Sukamto, J. H.; Orth, R. J.; Lilga, M. A.; Hallen, R. T. *Sep. Purif. Technol.* **1999**, *15*, 207−222.
(9) Lilga, M. A.; Orth, R. J.; Sukamto, J. P. H.; Haight, S. M.; Schwartz, D. T. *Sep. Purif. Technol.* **1997**, *11*, 147−158.
(10) Jeerage, K. M.; Schwartz, D. T. *Sep. Sci. Technol.* **2000**, *35*, 2375−2392.
(11) Lilga, M. A.; Orth, R. J.; Sukamto, J. P. H.; Rassat, S. D.; Genders, J. D.; Gopal, R. *Sep. Purif. Technol.* **2001**, *24*, 451−466.
(12) Jeerage, K. M. *Characterization of Electrodeposited Nickel Hexacyanoferrate for Electrochemically Switched Ion Exchange*; University of Washington: Seattle, 2001.
(13) Lasky, S. J.; Buttry, D. A. *J. Am. Chem. Soc.* **1988**, *110*, 6258−6260.
(14) Yu, Q.; Steen, W. A.; Jeerage, K. M.; Jiang, S.; Schwartz, D. T. *J. Electrochem. Soc.* **2002**, *149*, E195−E203.
(15) Jeerage, K. M.; Steen, W. A.; Schwartz, D. T. *Langmuir* **2002**, *18*, 3620−3625.
(16) Steen, W. A.; Han, S. W.; Yu, Q. M.; Gordon, R. A.; Cross, J. O.; Stern, E. A.; Seidler, G. T.; Jeerage, K. M.; Schwartz, D. T. *Langmuir* **2002**, *18*, 7714−7721.
(17) Loos-Neskovic, C.; Fedoroff, M.; Garnier, E. *Talanta* **1989**, *36*, 749−759.

10.1021/cm0217405 CCC: $25.00
Published on Web 05/21/2003

agitation.[17,18] To date, there has been no similar demonstration of material diversity in electroactive thin films of NiHCF. Thin films of NiHCF grown by anodic derivatization of nickel electrodes are normally reported to follow the redox stoichiometry

$$K_2NiFe(CN)_6 \leftrightarrow KNiFe(CN)_6 + e^- + K^+ \qquad (1)$$

when electrochemically modulated from the reduced (left) to the oxidized (right) forms in an alkali containing electrolyte (here potassium is shown), though this has not been explicitly confirmed.[1−7] The stoichiometry and structure of electroactive NiHCF thin films grown cathodically from marginally stable ferricyanide/nickelous sulfate solutions has been investigated using X-ray diffraction with corroborating X-ray spectroscopies (EXAFS and EDS). These methods show that cathodically deposited materials obey the redox stoichiometry

$$K_{1.33}Ni_{1.33}Fe(CN)_6 \leftrightarrow K_{0.33}Ni_{1.33}Fe(CN)_6 + e^- + K^+ \qquad (2)$$

with the ratio of nickel-to-iron going up due to $Fe(CN)_6^{-3/-4}$ vacancies from the unit cell, rather than added Ni.[16,19] The stoichiometry of redox reactions 1 and 2 can be generalized, on a unit cell basis, as

$$K_{8-4n-2m-(4-n)x}Ni^{II}{}_{4+m}[Fe^{II+x}(CN)_6]_{(4-n)} \qquad (3)$$

where n represents the average number of $Fe(CN)_6^{-3/-4}$ vacancies per unit cell ($0 \le n \le {}^4/_3$), m denotes the number of extra interstitial Ni^{II} in the unit cell ($0 \le m \le 4$), and x is the fraction of iron centers in the +3 oxidation state ($0 \le x \le 1$). Of course, the alkali cation stoichiometry must always remain non-negative, that is, $8-4n-2m-(4-n)x \ge 0$. Equation 3 shows that the effect of small nonstoichiometries in $Fe(CN)_6^{-3/-4}$ and/or Ni^{2+} are amplified in the stoichiometry of the intercalated alkali, especially for the oxidized solid ($x = 1$). Thus, the alkali content of the oxidized NiHCF matrix is a sensitive elemental probe of lattice nonstoichiometry.

Here, we demonstrate that the synthesis strategies used to create bulk NiHCF powders can be adopted to the synthesis of diverse electroactive thin films. Combinatorial synthesis and screening of electroactive compounds has most frequently involved the use of multielectrode arrays,[20−22] though the patterning of material libraries on a single-electrode substrate is gaining momentum.[23−26] The former approach is especially well suited to more focused studies, owing to the small library size possible with a microfabricated electrode array, whereas the latter approach is better for initial screening of larger libraries (so long as one has a nonelectrochemical method to probe individual library member). We demonstrate the patterning of a single electrode using the microdispensing of an aqueous divalent nickel source, a ferricyanide source, and a water diluent and show that mixing order (as in the bulk synthesis case) influences the diversity of the library. Raman spectroscopy is used to quantify the redox activity of individual library members, as we have described before,[27] and energy-dispersive X-ray spectroscopy (EDS) of intercalated cation is used to probe matrix nonstoichiometry.[10,14−16,19,27] The ability to synthesize diverse, electroactive NiHCF thin films is demonstrated.

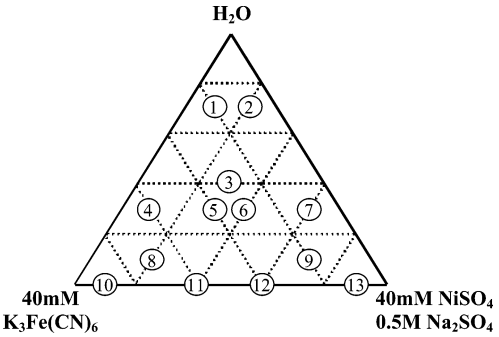

Figure 1. Ternary experimental design. Numbered locations correspond to the reagent volume percents used in each sample. A basis of 2 μL was used for each sample.

Experimental Section

Sample Preparation and Electrochemistry. Figure 1 shows a ternary diagram with varying volume percents of three source reagents Fe^{III} (40 mM $K_3Fe(CN)_6$), Ni^{II} (40 mM $NiSO_4$ and 0.5 M Na_2SO_4), and distilled H_2O. The reagent percents labeled 1−13 were chosen to assess the range of materials produced with this combinatorial approach. Although the supporting electrolyte (Na_2SO_4) affects solution conductivity and potentially film growth, it was only included in the Ni^{II} solution to keep this combinatorial route simple and straightforward (future experiments may account for this added variable, if needed).

Different NiHCF materials were nucleated and grown on the surface of a sandpaper-roughened (600 grit), electrochemically cleaned, 1-cm-diameter platinum disk electrode by pipetting 2 μL of each reagent mixture into 13 reagent wells. The 1-mm-diameter reagent wells were created using a laser-cut PVC tape mask. Details for creating and using laser-cut PVC tape masks are given elsewhere.[28] The platinum disk was roughened to improve mechanical adhesion of the film. The reagent mixing order was varied as follows:

Library A: $Fe^{III}/H_2O/Ni^{II}$ Library B: $Ni^{II}/H_2O/Fe^{III}$

The different combinations of Ni^{II}, Fe^{III}, and H_2O were deposited onto the substrates using a P2 Pipetman (Gilson International) in a room-temperature water-saturated environment. The samples were left in the water-saturated environment for several hours to ensure that water did not

(18) Loos-Neskovic, C.; Fedoroff, M.; Garnier, E.; Gravereau, P. *Talanta* **1984**, *31*, 1133−1147.
(19) Jeerage, K. M.; Steen, W. A.; Schwartz, D. T. *Chem. Mater.* **2002**, *14*, 530−535.
(20) Sullivan, M. G.; Utomo, H.; Fagan, P. J.; Ward, M. D. *Anal. Chem.* **1999**, *71*, 4369−4375.
(21) Siu, T.; Li, W.; Yudin, A. K. *J. Comb. Chem.* **2000**, *2*, 545−549.
(22) Jiang, R. Z.; Chu, D. *J. Electroanal. Chem.* **2002**, *527*, 137−142.
(23) Chen, G. Y.; Bare, S. R.; Mallouk, T. E. *J. Electrochem. Soc.* **2002**, *149*, A1092−A1099.
(24) Sun, Y. P.; Buck, H.; Mallouk, T. E. *Anal. Chem.* **2001**, *73*, 1599−1604.
(25) Gurau, B.; Viswanathan, R.; Liu, R. X.; Lafrenz, T. J.; Ley, K. L.; Smotkin, E. S.; Reddington, E.; Sapienza, A.; Chan, B. C.; Mallouk, T. E.; Sarangapani, S. *J. Phys. Chem. B* **1998**, *102*, 9997−10003.
(26) Reddington, E.; Sapienza, A.; Gurau, B.; Viswanathan, R.; Sarangapani, S.; Smotkin, E. S.; Mallouk, T. E. *Science* **1998**, *280*, 1735−1737.
(27) Steen, W. A.; Jeerage, K. M.; Schwartz, D. T. *Appl. Spectrosc.* **2002**, *56*, 1021−1029.
(28) Wang, W. H.; Holl, M. R.; Schwartz, D. T. *J. Electrochem. Soc.* **2001**, *148*, C363−C368.

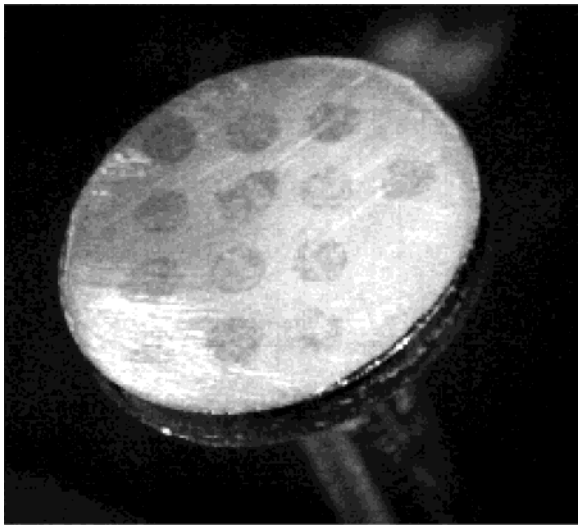

Figure 2. Photograph of a typical 1-cm-diameter Pt substrate with 13 separate 1-mm-diameter samples in an array.

evaporate from the mixtures while the NiHCF film nucleated and grew on the roughened electrode.

After film growth, the PVC-tape masks were removed and the libraries were cycled 15 times in a 1 M KNO_3 solution from 200 to 800 mV at 25 mV/s. The samples were then rinsed with distilled H_2O and cycled 15 more times in the same manner. The samples were placed in either the reduced (200 mV) or oxidized (800 mV) state by holding the potential for 15 min. All electrochemical experiments were performed using a PAR 273A Potentiostat, with potentials referenced to a saturated calomel electrode.

Figure 2 shows a photograph of a Pt substrate patterned in this manner. The 13 different 1-mm-diameter NiHCF library members are evident on the platinum disk substrate.

Raman Spectroscopy. The Raman spectroscopy system consisted of a Kr^+ laser tuned to 647.1 nm (Coherent Innova 90), a Spex 270M imaging spectrograph, and a Princeton Instruments CCD detector. Plasma emissions were removed from the laser line using an Omega Optical band-pass filter, and inelastically scattered light was collected from the sample at 90° from incident using a f/1.2 Nikon camera lens. The collected light was passed through an OD6 holographic notch filter before being focused into the spectrograph using an f/4 lens. A 200-μm slit and 1800 groove/mm grating were used. High signal-to-noise spectra were acquired between 30 and 300 s, depending on the amount of NiHCF material present. The spectral baseline was removed using a locally weighted least-squares regression technique before the spectra were area-normalized to account for differences in focusing and film thickness.

Energy-Dispersive X-ray Spectroscopy. A scanning electron microscope (JEOL JSM-5200) was operated at a 15-keV accelerating voltage to stimulate X-ray emissions. X-ray emissions with energies between 0 and 10 keV were collected using a Si(Li) detector with a Be window (Link Systems). Elements with $Z > 10$ were identified with this system. Spectra were acquired between 10 and 15 min, depending on the amount of material present. Spectral background was subtracted using a locally weighted least-squares regression technique, and the peaks were fit to a Gaussian function. All reported spectra were normalized using the Fe peak amplitude. Potassium was used as the intercalating cation for these studies because it has a strong EDS signal and no interference from other elements present in the system.

Results and Discussion

To create a material library, we varied the solution concentration and the mixing order for the ternary components described above and shown in Figure 1.

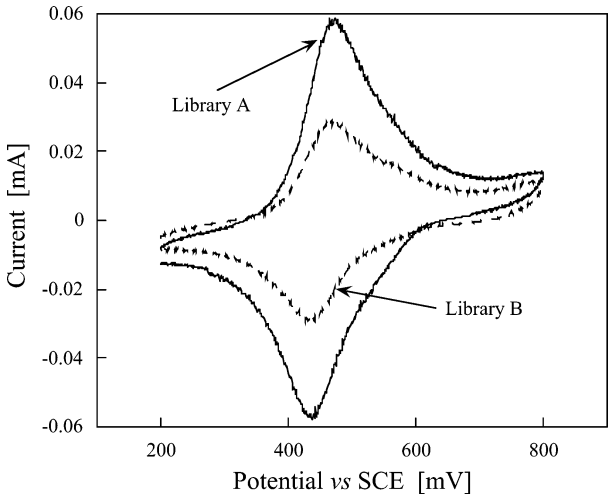

Figure 3. Composite cyclic voltammograms for Libraries A and B. The final CV is shown, with cycling performed in 1 M KNO_3 at 25 mV/s.

Mixing speed, temperature, pH, and substrate preparation were held fixed to simplify our strategy for creating a diverse electroactive thin film library. The rationale for selecting the two specific reagent mixing orders presented ($Fe^{III}/H_2O/Ni^{II}$ and $Ni^{II}/H_2O/Fe^{III}$), and for rejecting the other four possibilities ($H_2O/Fe^{III}/Ni^{II}$, $H_2O/Ni^{II}/Fe^{III}$, $Fe^{III}/Ni^{II}/H_2O$, $Ni^{II}/Fe^{III}/H_2O$), deserves more elaboration. Since water is a diluent and film growth does not occur until both transition metal reagents are added, the mixing orders $Fe^{III}/H_2O/Ni^{II}$ and $H_2O/Fe^{III}/Ni^{II}$ are identical, as are $Ni^{II}/H_2O/Fe^{III}$ and $H_2O/Ni^{II}/Fe^{III}$. We rejected the mixing orders $Fe^{III}/Ni^{II}/H_2O$ and $Ni^{II}/Fe^{III}/H_2O$ because the film-forming reaction would commence as soon as the second transition metal reagent was added. As a result, the exact nature of the final film would likely depend on the exact timing for the addition of water. This added constraint, though perhaps useful for building library diversity, would make eventual scaling of the process to larger libraries difficult. Thus, if we can demonstrate a diverse library without adding the diluent last, the synthesis will be more straightforward and scalable.

Figure 3 is a plot of the last cyclic voltammogram (CV) for Libraries A and B and shows that robust thin film libraries are produced. Cyclic voltammetry is a simple way to assess whether some or all of the library members are electroactive, but it does not address the electroactivity of individual members nor does it assess member diversity. Positive current in Figure 3 corresponds to the oxidation of NiHCF and K^+ deintercalation out of the matrix. Negative current denotes reduction and K^+ intercalation back into the NiHCF matrix. The CVs for Libraries A and B represent the superposition of all the electroactive library members. Library A clearly has the higher average capacity, which may indicate more members are electroactive or that mixing order A results in thicker films. The higher currents could also be due to Library A having, on average, more members with stoichiometries closer to $n \approx m \approx 0$ in eq 3.

The electroactivity of individual library members was explored using Raman spectroscopy. Both libraries were electrochemically reduced and ex situ Raman spectra were taken of all 26 members; the libraries were then

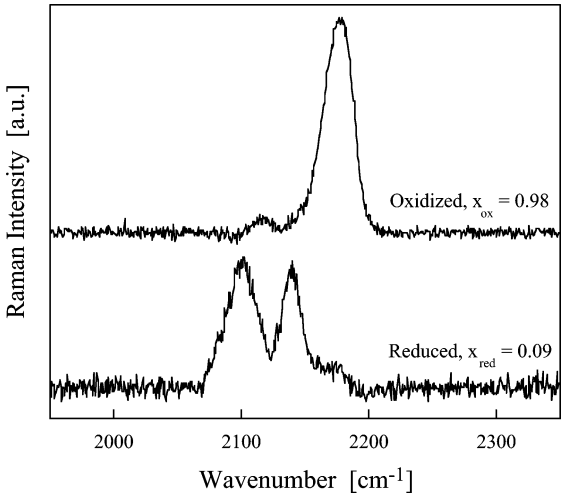

Figure 4. Representative Raman spectra of NiHCF for sample A1 in the oxidized and reduced states. The values labeled x_{ox} and x_{red} quantify the fraction of iron centers in the +3 valence state for the oxidized and reduced samples, respectively, based on a multivariate regression model detailed elsewhere.[27]

oxidized and spectra were again acquired. Figure 4 shows representative cyanide stretching spectra for member 1 of Library A (referred to as Sample A1). The two low wavenumber peaks (ca. 2100 and 2140 cm^{-1}) in the lower spectrum are representative of cyanide stretching in the vicinity of Fe^{II} while the upper spectrum with its single, higher wavenumber peak (ca. 2175 cm^{-1}) is representative of cyanide near Fe^{III}. Multivariate analysis is used to calculate the fraction of Fe in the +3 state (i.e., the variable x in eq 3).[27,29] The values of x shown in Figure 4 for Sample A1 (i.e., $x_{red} = 0.09$ and $x_{ox} = 0.98$) prove that this library member is quite electroactive, with 89% of all irons ($\Delta x = 0.98-0.09$) switching between the reduced and oxidized states. The most electroactive materials have $\Delta x = 1$; inactive members have Δx approaching 0. Raman spectroscopy was used to eliminate 5 inactive members from Library A and 6 from Library B. What remains are 8 electroactive members in Library A and 7 in Library B, which is consistent with the larger currents observed in Figure 3 for Library A (though not in direct proportion).

The reagent compositions that produce electroactive and inactive members in both libraries are shown schematically in Figure 5. Larger circles correspond to greater electroactivity (i.e., circle diameter increases as Δx increases). Inactive samples are denoted by an "**X**". The ternary diagrams for the two libraries are plotted edge-to-edge to better show symmetry in the synthesis conditions. Figure 5 shows that four of the five inactive members in Library A are also inactive in B, with high nickel growth conditions leading to the majority of inactive members. The values of Δx for all electroactive members are >0.7 with most approaching 1.

Oxidized state EDS spectra of the 8 remaining electroactive members from Library A are shown in Figure 6a. Spectra for the 7 remaining samples from Library B are shown in Figure 6b. Each spectrum in Figure 6

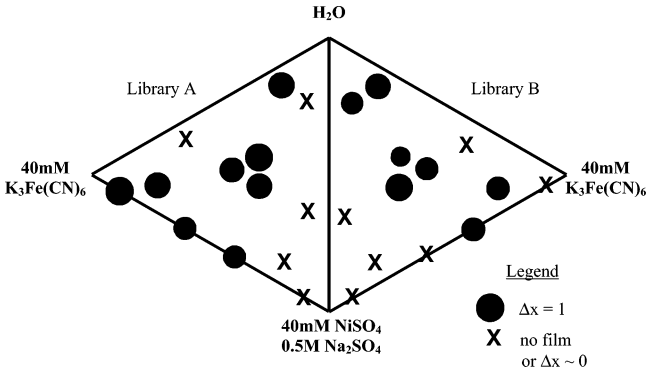

Figure 5. Redox activity for Libraries A (left) and B (right). The diameter of the black dots is proportional to Δx (see legend). The ternary diagrams are positioned with a common edge to better illustrate the processing symmetry in the two Libraries.

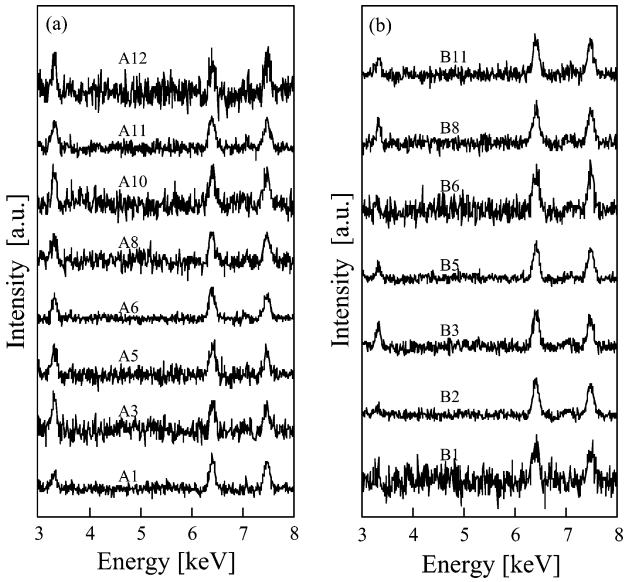

Figure 6. Fe-normalized EDS spectra for the electroactive samples in Library A (a) and Library B (b). The K peak is at 3.3 keV, Fe is at 6.4 keV, and Ni is at 7.5 keV.

is normalized to give identical integrated Fe peak intensities (at 6.4 keV). By normalizing with respect to Fe intensity (the films redox centers), the influence of film thickness is removed, so long as all the films are thin compared to the penetration depth of the electron beam.[10,19] In all the spectra, a dominant Pt substrate signal was seen at ~2 keV, indicating the NiHCF films were indeed thin (not shown, since it dwarfs all other peaks). The peak at 3.3 keV corresponds to intercalated K ions while the peak at 7.5 keV is from Ni. In this thin film limit, the ratio of K-to-Fe peak intensity (I_K/I_{Fe}) is proportional to the unit cell stoichiometry for K intercalated into the matrix.

As noted in the Introduction, eq 3 shows that small variations in matrix stoichiometry (n and m) are amplified in the intercalated cation stoichiometry. Thus, I_K/I_{Fe} is a straightforward probe of lattice nonstoichiometry, with variations in the oxidized state K content being the simplest measure of material diversity. Figure 6a shows that all of Library A's members display appreciable K intensity in the Fe-normalized EDS spectra, but A3, A10, and A12 are more than twice as big as A1. On the other hand, most of Library B's members (Figure

(29) Haight, S. M.; Schwartz, D. T.; Lilga, M. A. *J. Electrochem. Soc.* **1999**, *145*, 1866−1872.

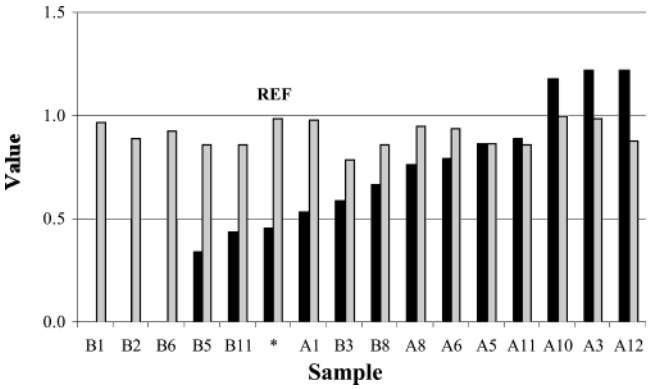

Figure 7. Plot of I_K/I_{Fe} (black bars) and x_{ox} (gray bars) for every electroactive sample in Libraries A and B, and a reference sample of known stoichiometry and structure. The reference sample, denoted by ∗ and labeled REF, has been analyzed elsewhere using EDS, Raman, X-ray diffraction, and extended X-ray absorption fine structures.[16,19] Samples to the left of REF have a more nonstoichiometric matrix and vice versa for those to the right.

6b) are smaller than A1. In fact, members B1, B2, and B6 have extremely small amounts of intercalated K. Despite the small library size, the wide range of Fe-normalized K EDS intensities seen in Figure 6 reflects a substantial amount of stoichiometric diversity.

It is worthwhile gaining a more quantitative appreciation for the stoichiometric diversity in this library. Figure 7 is a plot of I_K/I_{Fe} (black bars) and x_{ox} (gray bars) for all electroactive samples and a fully characterized reference sample (denoted REF, described below). Most samples approach a fully oxidized state (i.e., $x_{ox} \rightarrow 1$), a fact that could be surmised from Figure 5. For a perfectly oxidized sample with $x = 1$, eq 3 gives the number of K^+ ions per unit cell as $N_{K,ox} = 4 - 3n - 2m$. We have shown using EDS, X-ray diffraction (XRD), and extended X-ray adsorption fine structure (EXAFS) that cathodically deposited NiHCF thin films have values of $n \approx 1$ and $m \approx 0$, yielding $N_{K,ox} \approx 1$ and the number of irons per unit cell as $N_{Fe} = 3$.[16,19] The Fe-normalized EDS signals for oxidized NiHCF thin films made by cathodic deposition is labeled REF in Figure 7 and is near $I_K/I_{Fe} \approx 0.5$.[19] Since I_K/I_{Fe} is linearly proportional to $N_{K,ox}/N_{Fe}$ for a thin film, we have sufficient information about REF to find the constant of proportionality, that is, $I_K/I_{Fe} \approx 1.5*N_{K,ox}/N_{Fe}$. In general, eq 3 shows that $N_{K,ox}/N_{Fe} = (4 - 3n - 2m)/(4 - n)$ for an oxidized matrix. As a result, library members with I_K/I_{Fe} too small to be accurately fit (B1, B2, B6) have $N_{K,ox}/N_{Fe} \approx 0$, meaning the maximum possible matrix nonstoichiometry (i.e., $3n + 2m \approx 4$). On the other hand, a perfectly stoichiometric matrix ($n = m = 0$) yields $N_{K,ox}/N_{Fe} = 1$ and an intensity ratio $I_K/I_{Fe} \approx 1.5$. Figure 7 shows that the largest intensity ratios we observe (A3, A10, A12) are near $I_K/I_{Fe} \approx 1.25$. Thus, our small library has a great deal of diversity, but seems to miss those electroactive NiHCF thin films for which $3n + 2m \leq 1$ (or, $N_{K,ox} \geq 3$). These results, namely, the higher matrix nonstoichiometries in Library B compared to those in A, are also consistent with the lower currents seen in the composite CV for Library B (Figure 3). For films of a given thickness, a higher matrix nonstoichiometry means fewer electrons are transferred (lower current) because fewer alkali cations are intercalated/deintercalated. In short, the composite response of the libraries is entirely consistent with the number of electroactive members in each library and the overall differences observed in their level of matrix nonstoichiometry.

Concluding Remarks

A route for synthesizing a diverse combinatorial library of electroactive NiHCF thin films was demonstrated, with Raman spectroscopy and EDS providing the evidence for this diversity. Though not explored further, the synthesis approach described here uses fairly mild conditions and appears well-suited for scaling to much larger libraries. For example, others have patterned conductive carbon paper substrates by direct ink jet printing of reagent mixtures;[26] this should be possible here since electroactive metal hexacyanoferrates have been shown to grow on carbon supports.[30] Ink jet printing would remove the need to create a PVC tape mask to define reagent wells and smaller drops would mix more quickly, leading to more reproducible film growth conditions.

It is also worth noting that a number of the library members completely (or, almost completely) deintercalate their cations upon oxidation. This trait, which has not been observed before in an electroactive NiHCF thin film, is an extremely desirable property for the efficient regeneration of the matrix when used for cation separations. Thus, the ability to make a diverse library of stoichiometric/structural variants appears to create opportunities for developing better electrochemical sensor and separation materials. Focused characterization of the selectivity traits and cycle life of promising variants is necessary for achieving this goal.

Acknowledgment. The authors gratefully acknowledge support provided by National Science Foundation Grant No. CTS-0236608.

CM0217405

(30) Green-Pedersen, H.; Korshin, G. V. *Environ. Sci. Technol.* **1999**, *33*, 2633−2637.